Synthesis and Properties of Novel Ruthenium Thin-Film Materials: Self-Assembled Multilayer Approaches

DeQuan Li,* David C. Smith, and Basil I. Swanson*

Inorganic and Structural Chemistry (INC-4), Los Alamos National Laboratory, Los Alamos, New Mexico 87545

J. D. Farr and M. T. Paffett

Surface and Microanalysis (CLS-1), Los Alamos National Laboratory, Los Alamos, New Mexico 87545

M. E. Hawley

Polymers and Coatings (MST-7), Los Alamos National Laboratory, Los Alamos, New Mexico 87545

Received March 24, 1992. Revised Manuscript Received May 25, 1992

The synthesis and characterization of stable ruthenium thin films via low-temperature, aqueous solution techniques where self-assembled monolayers are employed to enhance adhesion are described. A monolayer of *N*-[3-(trimethoxysilyl)propyl]ethylenediaminetriacetate (TMPEDTA) was first introduced onto the surface of fused-silica by a self-assembling scheme followed by nonelectrolytic deposition of a ruthenium thin film using $Ru(H_2O)_6^{2+}$. The metallic Ru thin films have been characterized by Rutherford backscattering (RBS), electron microprobe analysis (EMPA), scanning electron microscopy (SEM), and scanning tunneling microscopy (STM). RBS suggests a typical thickness of 1500 Å for these Ru mirror samples, and STM indicates that the surface morphology has 10–25-nm structural domains. In addition, X-ray photoelectron spectroscopy (XPS), secondary ions mass spectroscopy (SIMS), and Auger photoelectron spectroscopy (AES) were carried out to elucidate the chemical compositions of these Ru mirror thin films. XPS, SIMS, and AES indicate that the Ru mirror films mainly contain ruthenium metal with 10–20% concentration of oxygen as the sub-oxide RuO.

Introduction

The design, construction, and molecular architecture of artificial, supermolecular, self-assembled lattices with planned structures and physical properties has attracted recent interest.[1-5] Covalently bound self-assembled monolayers[6] or multilayers,[7] such as alkylsilanes on glass or alkylthiols on gold, offer a potential starting point for fabricating highly ordered multifunctional thin films. Applications include covalently bound multilayers for nonlinear optical materials.[8-10] The central advantage of using covalently bound self-assembly schemes is that the weak physical interactions between interfaces, as in the case of Langmuir–Blodgett films, are replaced with covalent bonds. Moreover, the film thickness and coverage is extremely uniform since the surface functional groups are uniformly distributed and, as soon as the surface functional groups are consumed, the surface reaction stops, eliminating excess deposition. Novel metal complexes can be constructed on the surface of various oxides by first introducing/incorporating covalently bound, self-assembled monolayers or multilayers of multidentate ligands as anchors for transition-metal ions. This strategy offers the capability of studying the novel properties of inorganic metal complexes in the environment of self-assembled arrays of monolayers or multilayers. We have now used covalently bound, self-assembled monolayers at the interface between an oxide substrate and a metal thin film to enhance adhesion properties.

There has been great interest in generating ruthenium and ruthenium oxide or sub-oxide thin films. The mixed RuO_2 and TiO_2 system as a catalyst for chlorine evolution has been successfully employed for more than two decades.[11] The success of this catalyst is due to the excellent electrocatalytic properties of RuO_2 and its strong coupling to TiO_2. In addition, semiconducting TiO_2 materials are considered as candidates for photoelectrochemical energy conversion. Unfortunately, the large bandgap and low conductivity of TiO_2 make solar energy conversion efficiency too small for commercial usage.[12] RuO_2-modified TiO_2 materials, however, show increased photocurrents as a result of the shift of the photoresponse toward the visible.[13] More recently, new chemical sensors utilizing magnetic semiconductive thick-film containing ruthenium sub-oxides (RuO) have been reported.[14] These chemical sensors, which are based on a linear change in resistance, are sensitive to alcohol, acetone, and ammonia. The relationship between the resistivity and the chemical vapor concentration is linear from a few ppm up to approximately 5000 ppm.

Combining self-assembly chemistry and a thermally induced deposition technique, we report the preparation and properties of covalently bonded, self-assembled

(1) Lee, H.; Kepley, L. J.; Hong, H. G.; Mallouk, T. E. *J. Am. Chem. Soc.* **1988**, *110*, 618–620.
(2) Ulman, A.; Tillman, N. *Langmuir* **1989**, *5*, 1418–1420.
(3) Pomerantz, M.; Segmuller, A.; Netzer, L.; Sagiv, J. *Thin Solid Films* **1985**, *132*, 153–162.
(4) Putvinski, T. M.; Schilling, M. L.; Katz, H. E.; Chidsey, C. E. D.; Mujsce, A. M.; Emerson, A. B. *Langmuir* **1990**, *6*, 1567–1571.
(5) Allara, D. L.; Atre, S. V.; Elliger, C. A.; Snyder, R. G. *J. Am. Chem. Soc.* **1991**, *113*, 1852–1854.
(6) Wasserman, S. R.; Tao, Y. T.; Whitesides, G. M. *Langmuir* **1989**, *5*, 1074–1087.
(7) Maoz, R.; Sagiv, J. *J. Colloid Interface Sci.* **1984**, *100*, 465–496.
(8) Li, D.; Ratner, M. A.; Marks, T. J.; Zhang, C.; Yang, J.; Wong, G. K. *J. Am. Chem. Soc.* **1990**, *112*, 7389–7390.
(9) Dai, D.; Hubbard, M.; Li, D.; Park, J.; Ratner, M. A.; Marks, T. J.; Yang, J.; Wong, G. K. In *ACS Symp. Ser.; New Materials for Nonlinear Optics*; American Chemical Society: Washington, DC, **1991**; No. 455, pp 226–249 (Boston, MA, Apr 1990).
(10) Li, D.; Marks, T. J.; Zhang, C.; Yang, J.; Wong, G. K. Nonlinear Optical Properties of Organic Materials III; *SPIE Proc.* **1990**, *1337*, 341–346.
(11) Nidola, A. In *Electrodes of Conductive Metal Oxides*; Trasatti, S., Ed.; Elsevier: Amsterdam, 1981; Vol. B.
(12) Kozlowski, M. R.; Tyler, P. S.; Smyrl, W. H.; Atanasoski, R. T. *J. Electrochem. Soc.* **1989**, *136*, 442–450.
(13) Kawai, T.; Skata, T. *Chem. Phys. Lett.* **1980**, *72*, 87.
(14) Seki, K.; Shida, J.; Matsuki, H.; Murakami, K. *IEEE Trans. Magn.* **1990**, *26*, 2035–2037.

0897-4756/92/2804-1047$03.00/0

monolayers of *N*-[3-(trimethoxysilyl)propyl]ethylenediaminetriacetate (TMPEDTA) and the formation of a ruthenium mirror multilayer thin film on top of this multidentate ligand monolayer.

Experimental Section

All procedures are carried out under an argon atmosphere. Solvents were degassed by pumping under vacuum 1 h before use. All solutions are aqueous unless otherwise noted. The fused quartz substrates were ultrasonically cleaned in 10% detergent solution for 10 minutes and then refluxed in 1% tetrasodium ethylenediamine tetraacetate solution for 10 min followed by another 10-min sonication at ambient temperature. Finally, the substrates were thoroughly rinsed with deionized water and acetone and then exposed to argon plasma at 0.5 Torr for more than 0.5 h. Polished Si wafers were cleaned by sonicating in 10% detergent solution for 10 min and then exposed to argon plasma for 30 min. All substrates were used immediately after cleaning.

Synthesis of $[Ru^{II}(H_2O)_6]$·2tos. The hexaaquaruthenium(II) complex was synthesized according to a slightly modified literature procedure.[15,16] To RuO_2 (2.5 g) in an argon-purged system, $NaIO_4$ (12.5 g) and ice-cold H_2SO_4 (50 mL, 50%) were added. The volatile product, RuO_4, was then swept into two consecutive 1 M H_2SiF_6 baths with a total volume of 200 mL containing activated Pb of 17.5 and 5 g, respectively. After 2 days, the aqueous H_2SiF_6 baths turned purple, indicating formation of $[Ru^{2+}(H_2O)_6]\cdot[SiF_6]$. The Pb^{2+} was removed by addition of 2 M H_2SO_4 (50 mL) followed by filtration. The resulting purple solution was diluted and loaded onto a Dowex W50X8 column which was thoroughly washed with 1 M HCl, H_2O, and 0.1 M Htos (Htos = *p*-toluenesulfonic acid) sequentially. The product eluted with 1.8 M Htos solution. The red-purple solution was concentrated under vacuum at ~30 °C. Upon cooling, the $[Ru^{2+}(H_2O)_6]$·2tos was obtained and rinsed with excess ethylacetate to remove the Htos residue.

Caution: All operations were carried out in a well ventilated hood because of the toxicity and volatility of RuO_4.

Formation of TMPEDTA Monolayer on the Surface of Fused-Quartz Substrates. A *cleaned* SiO_2 substrate was incubated at pH = 2–3 (adjusted with concentrated HCl, a catalyst for Si–OMe bond hydrolysis) with a 5.0×10^{-3} M *N*-[3-(trimethoxysilyl)propyl]ethylenediaminetriacetate (TMPEDTA) solution at 70 °C for 3 days. The reaction vessel was designed in such a way so that sufficient open space is available at the surface of the substrates to allow smooth and continuous diffusion of the solution species onto the surface. After 3 days, the system was allowed to slowly cool to room temperature. After thoroughly rinsing with deionized water, the fused-quartz substrate was immersed in a 0.1 M pH = 5.5 HAc/KAc buffer for 2–3 h with 10 min of gentle sonication every 30 min. The multidentate ligand TMPEDTA modified substrates were then sonicated (1 min) in water three times and thoroughly rinsed with water and acetone. The coated substrates were allowed to dry in air.

Formation of TMPEDTA Monolayer on the Surface of Silicon Substrates. A *cleaned* Si wafer was heated at pH = 2–3 with a 5.0×10^{-3} M *N*-[3-(trimethoxysilyl)propyl]ethylenediaminetriacetate (TMPEDTA) solution at 70 °C for 3 days. After 3 days, the Si wafer coated with monolayer of multidentate ligand TMPEDTA was then cleaned by sonication (1 min) in water three times and finally rinsed with water thoroughly, followed by acetone for quick drying in air.

Low-Temperature (<50 °C) Ru Mirror Formation. The covalently modified TMPEDTA fused-quartz substrate was immersed in a 10-mL degassed solution of $Ru(H_2O)_6^{2+}$ (3.6×10^{-2} M) in a water bath. It is necessary to have sufficient radial volume of solution to allow continuous/smooth diffusion of $Ru(H_2O)_6^{2+}$ to the substrate surfaces in order to form uniform shiny films. The temperature of the purple $Ru(H_2O)_6^{2+}$ solution was slowly increased to 40 °C and allowed to slowly cool to 35 °C before the next cycle of heating was started. The cyclic heating process was maintained overnight. After the completion of the above steps, a shiny, smooth, metallic-looking mirror was formed on the quartz substrate.

Surface Analysis. Auger electron spectroscopy (AES) and X-ray photoelectron spectroscopy (XPS) were performed with commercial cylindrical mirror electron energy analyzers. Electron beam conditions for AES were typically 3 keV and 1 nA total beam current in a spot size 0.1 mm^2. X-ray irradiation for XPS was performed using an achromatic Mg source ($h\nu$ = 1253.6 eV). Narrow scans were performed with a band pass of 50 eV, and satellite and inelastic background were removed from spectra using established procedures.[17] AES depth profiling was performed using 3-keV Ar ions with a nominal sputter removal rate of ~100 Å min^{-1} for Ru. Secondary ion mass spectroscopy (SIMS) was performed in both static and dynamic modes using either 5-keV Ar or Xe mass-filtered ion beams of appropriate beam current density. Mass analysis of the sputtered material was performed using a quadruple instrument with provision for detection of positive, negative, and sputtered neutral species. Insulating surfaces (e.g., quartz substrates) were examined using appropriate application of a low-energy ($E_i \leq 100$ eV) electron source for both SIMS and XPS.

Scanning electron micrographs (SEM) were obtained in a Hitachi S520-LB scanning electron microscope. A Microspec WDX-2A wavelength spectrometer was used to quantitatively measure both Ru and C. An accelerating voltage of 10 kV and a takeoff angle of 70° were used to minimize corrections to the raw data. The beam was rastered over an area of roughly 200–400 μm^2 to further reduce the current density and minimize carbon deposition. The total current to the sample was generally less than 30 nA. Variations in electron beam intensity were corrected for by use of Faraday cup measurements. Pure element standards were used to provide reference intensity measurements for Ru and C. A local version of the program CITPTC was used to provide quantitative corrections. This program integrates the X-ray depth distribution function ($\phi(\rho z)$) to determine the composition of films whose thickness is less than the electron range.

The STM constant-current images were taken under ambient conditions with a Nanoscope II using cold worked PtIr scanning probes. No special preparation to the films surface was required to obtain the pictures presented in this paper. Electrical connection to the samples was made with Ag colloidal paint and the average bias voltage applied to the sample was about 700–800 mV at typical set point current settings of 0.07–0.10 nA. To minimize image distortion, scan speeds were generally kept below 2 Hz.

Rutherford backscattering (RBS) analyses were obtained with the 3MV tandem accelerator at the Ion Beam Materials Laboratory at Los Alamos National Laboratory using a beam of He^+ of energy of 2.2 MeV.

The infrared of both TMPEDTA monolayer and Ru mirror films was performed on Bio-Rad FTS-40 with Harrick Seagull variable-angle reflection attachment. The TMPEDTA monolayer was studied using the internal total reflection mode in which the Si wafer functionalized with a monolayer TMPEDTA was pressed against a ZnSe hemisphere crystal with a miniature pressure device to assure optical contact. A single attenuated total reflection from the interface of ZnSe crystal and TMPEDTA/Si was collected with 64 scans and 2-cm^{-1} resolution. Details of the experimental setup will be discussed elsewhere.[18] The metallic Ru mirror films were studied using the external reflection mode at 45° of incident because the films reflect infrared radiation perfectly.

Results and Discussion

The synthetic approach is summarized in Scheme I. A monolayer of TMPEDTA, a multidentate ligand, was introduced onto a *cleaned* fused quartz/silicone wafer surface via a siloxane bond linkage. This procedure was accomplished by incubating the freshly cleaned fused-quartz substrate in a slightly acidic 5.0×10^{-3} M TMPEDTA aqueous solution at 70 °C for a few days. In acidic aqueous solution, covalent binding[19] of monofunctional silanols to

(15) Bernhard, P.; Biner, M.; Ludi, A. *Polyhedron* **1990**, *9*, 1095–1097.
(16) Bernhard, P.; Burgi, H.; Hauser, J.; Lehman, H.; Ludi, A. *Inorg. Chem.* **1982**, *21*, 3936–3941.
(17) Storer, R. A. In *ASTM Standards on Surface Analysis*; American Society for Testing and Materials: Mars, PA, 1986; pp 17–21.
(18) Li, D.; Swanson, B. I., manuscripts in preparation.
(19) Haller, I. *J. Am. Chem. Soc.* **1978**, *100*, 8050.

Scheme I

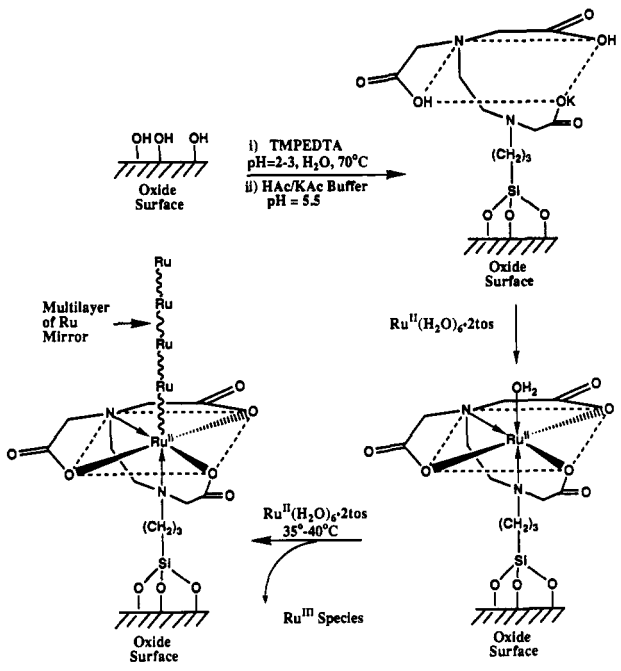

oxide surfaces competes with dimerization to form the corresponding (unreactive) siloxane, and it has been suggested that a reasonably compact monolayer of silane is formed under these conditions.[20] The absorptions at 213 and 277 nm are consistent with monolayer coverage on fused quartz. A single attenuated internal total reflection (ATR) from Si wafer surface shows a C=O stretch at 1730 cm^{-1} and two CH_2 bands at 2848 and 2924 cm^{-1} (shoulder at 2957 cm^{-1}) corresponding to the $\nu_s(CH_2)$ and $\nu_a(CH_2)$ vibrations, respectively. The TMPEDTA layer was functionalized with Ru by reaction with $Ru^{2+}(H_2O)_6$·2tos at room temperature. Throughout this reaction, the monolayer surface was maintained at pH ≈ 5.5 by preimmersing the ligand-functionalized substrate in an HAc/KAc (0.1 M) buffer solution for 2–3 h; this helps to avoid degradation reactions of the $Ru^{2+}(H_2O)_6$ reagent. The compound $Ru^{2+}(H_2O)_6$ is most stable in a slightly acidic medium and readily decomposes in alkaline solution.

When the TMPEDTA monolayer, buffered at pH ≈ 5.5, was heated to 35–40 °C (see Experimental Section) in a $Ru^{2+}(H_2O)_6$ solution, a shiny, conductive (ρ = 57.5 Ω/cm) film was formed on the TMPEDTA covalently attached adhesion layer. The conductivity data were obtained by two-point measurements. The relatively low conductivity may be a result of probe contact resistances. Excluding surface contamination, there are only two elements present in the conductive film as suggested by XPS, AES, and SIMS, i.e., 80–90% ruthenium and minor amount of oxygen (10–20 atomic wt %). The source of oxygen is not clear and can be probably explained by the ruthenium film absorbing oxygen or water from air or solution and hence forming ruthenium surface contaminant. No evidence has been found for the existence of RuO_2 in the metallic film from XPS, AES, and SIMS measurements, but sub-oxide RuO mass was detected by SIMS technique. Both ruthenium and ruthenium oxides are good conductors; therefore, one cannot distinguish between the two chemical compositions by conductivity measurements.

The formation of metallic thin films containing both ruthenium and oxygen can be explained by either one of

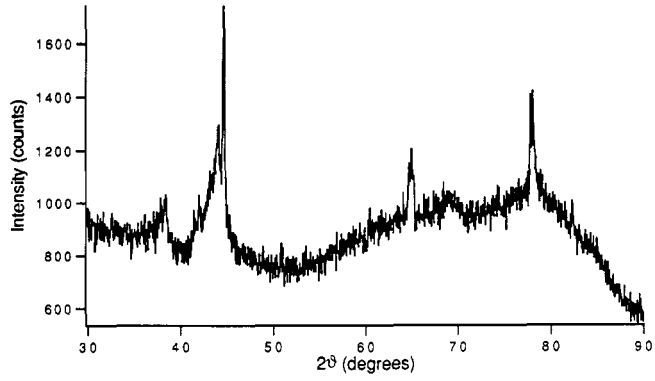

Figure 1. X-ray diffraction pattern of a metallic ruthenium thin film on a fused-quartz substrate.

the following Ru^{2+} thermal induced disproportionation reactions, i.e. (1) and (2).

$$3Ru(H_2O)_6^{2+} \rightarrow Ru(surf.) + 2Ru(H_2O)_6^{3+} + 6H_2O \quad (1)$$

or

$$2Ru(H_2O)_6^{2+} \rightarrow Ru(surf.) + RuO_2 + 4H^+ + 10H_2O \quad (2)$$

Thermodynamically, the standard reduction potential change for reaction 1 is ΔE = –0.043 V based on the data given by Greenwood and Earnshaw.[21] Similarly, the change of standard reduction potential for reaction 2 is ΔE = –0.665 V. From the above analyses, the reverse reaction of eq 2 is thermodynamically favorable whereas reaction 1 is extremely close to equilibrium under standard conditions (i.e., $\Delta G°$ = 0) and very likely to proceed in the forward direction given the slightly different conditions such as the elevated temperature, proper pH, and concentration. We conclude, therefore, that the Ru mirror film formation is driven primarily by reaction 1 as this would also account for the low oxygen concentration found in these metallic films. In addition, the ruthenium to oxygen ratio would be exactly 1 if reaction 2 occurred on the surface of covalently bound multidentate TMP(EDTA)Ru^{2+} self-assembled metal complex monolayer. Moreover, the oxygen content should be uniform throughout the metallic films, which is to the contrary of AES and SIMS profile results which show a decreasing oxygen concentration as the outer layers are sputtered away.

X-ray powder diffraction was performed on these ruthenium thin films and it shows the metallic films are weakly crystalline (see Figure 1). Most of the diffraction peaks match well with the theoretical prediction of pure ruthenium (2θ = 38.4, 42.0, 44.0, 77.8, and 82.4°). There are three additional diffraction lines, however, at 2θ values of 44.7, 65.1, and 78.1° which do not match the diffraction pattern of pure ruthenium metal. None of the above observed peaks matches the values reported for RuO_2. There is no reported X-ray powder diffraction data for RuO. The fused-silica substrates used are completely amorphous in this region (2θ = 30–90°). These diffraction results suppport the above analysis: i.e., Ru^{2+} disproportionation into Ru metal and Ru^{3+} followed by absorption of oxygen/water by the ruthenium metallic film from exposure to aqueous solution and ambient air to form surface contaminants possibly including sub-oxide RuO or/and Ru aqua complex $Ru(H_2O)_x$. Furthermore, the resulting solution from the ruthenium film formation is yellow and subsequently turns black upon standing in air; this be-

(20) Lee, H.; Kepley, L. J.; Hong, H. G.; Akhter, S.; Mallouk, T. E. *J. Phys. Chem.* 1988, *92*, 2597–2601.

(21) Greenwood, N. N.; Earnshaw, A. In *Chemistry of the Elements*; Pergamon Press: New York, 1989; pp 1242–1290.

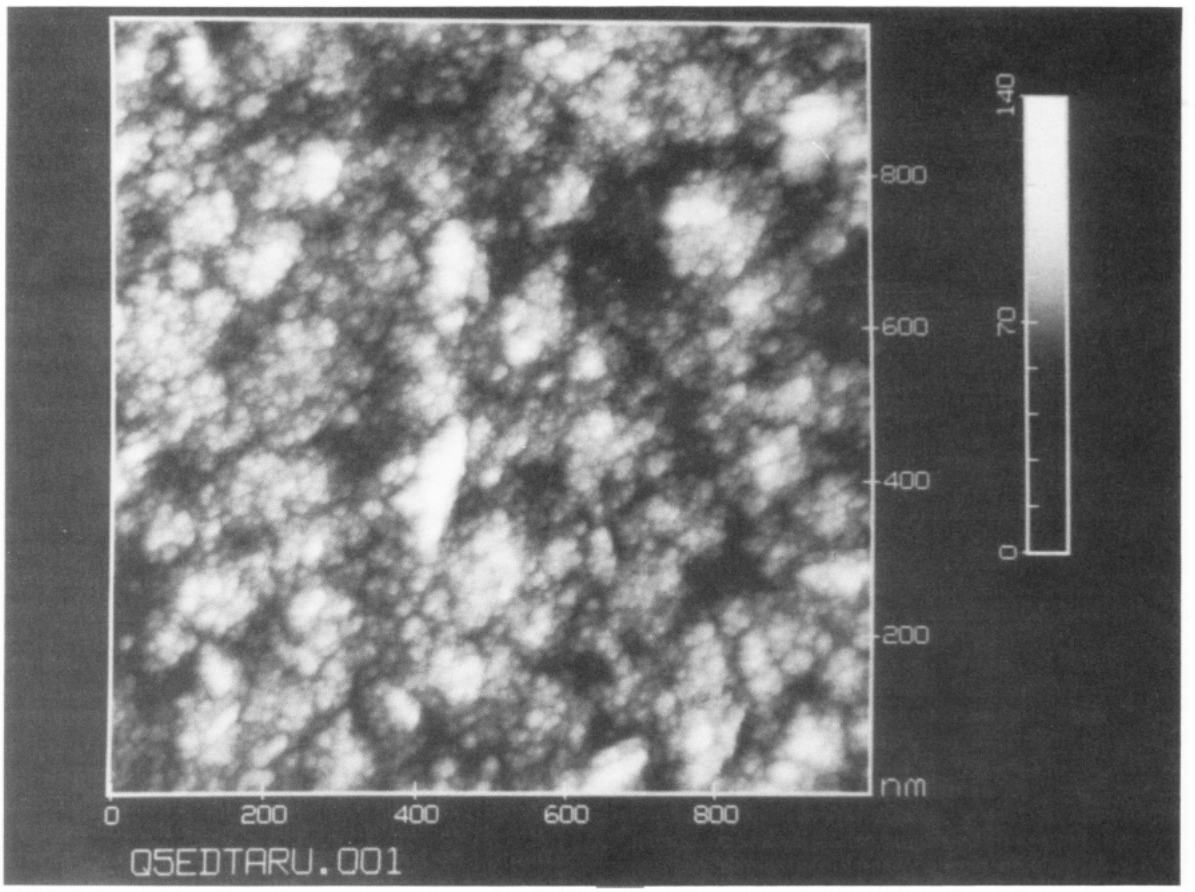

Figure 2. Top view STM constant-current image of a 1 μm × 1 μm area of Ru thin film measured in air showing relatively smooth surface on the micrometer scale. Sample bias of 750 mV and set point current of 100 pA were used.

havior is also observed for Ru^{3+} species, $Ru(H_2O)_6^{3+}\cdot 3tos$, under the same conditions.

The monolayer of TMPEDTA functions as an adhesion layer to enhance the formation of robust metallic ruthenium mirror films. Ruthenium also deposits on substrates which do not have the monolayer of TMPEDTA, but the metallic thin films fall off from the substrate readily. Metallic mirrors formed on top of TMPEDTA show strong adhesion to the substrates and can tolerate short period of plasma radiation and sonication.

Infrared studies of matrix-isolated ruthenium oxides (RuO_2 and RuO_3) and sub-oxide (RuO) have been reported[22] and the ruthenium oxides have characteristic vibration bands at 834 cm^{-1} for RuO, 902 cm^{-1} for RuO_2, and 893 cm^{-1} for RuO_3. FTIR external reflection spectroscopy was carried out on these ruthenium mirror thin films with a variable-angle reflection Seagull attachment and no detectable amount of ruthenium oxides, RuO, RuO_2, or RuO_3, was observed. The infrared result agrees well with the reported ruthenium properties, which indicates that ruthenium metal is stable to atmospheric attack and is virtually unaffected by non-oxidizing acids or even aqua regia. The infrared suggests that the metallic films consist mainly of Ru metal and the amount of oxygen is under the detection limit (i.e., <10–20%) of the infrared instrument if any oxygen is present as the suboxide. This observation was also confirmed by the XPS, SIMS, and AES results.

Scanning electron micrographs (×5.0K) reveal these films to be quite smooth with only a few agglomerate structures on the surface. At higher magnifications (× 20.0K) some surface grain structure is observed with a few pits and pin holes.

Scanning tunneling microscope images of the ruthenium film were taken at a series of progressively increasing resolutions. The STM data reveal a relatively smooth surface with a typical standard deviation roughness of about 10 nm for a 1 × 1 μm^2 scan as illustrated in Figure 2. It is clear from this figure that the surface roughness is due to a granularity of the film which consists of several orders of hierarchical structure. At the lowest resolution 100–150-nm circular rounded domains are observed. At an intermediate resolution, these domains are seen to consist of 10–25-nm-diameter subunits as shown in Figure 3. A software generated 30° profile rendering of a 50 × 50 nm^2 scan is presented in Figure 4. Finer substructure is clearly resolved within each subunit with dimensions of the order of 20 Å. Though the film is certainly not 100% "crystalline", i.e., well-oriented subunits, there does exist some short-range order which can be seen in the micrographs presented in Figures 3 and 4. This result is in good agreement with the X-ray diffraction pattern which also suggests a weakly crystalline ruthenium thin film. The surface of the ruthenium film was sufficiently conductive to easily obtain good-quality moderate resolution STM data, but attempts at near atomic resolution were unsuccessful. It is likely that, since the imaging was carried out in air, the presence of surface contaminants, oxides, and adsorbates determined the final resolution limitation.

A typical RBS spectrum of the ruthenium metallic thin film is given in Figure 5 indicating the presence of mainly Ru in the film along with Si and O from the fused quartz. Film thicknesses of ~1500 Å were measured by RBS. Depth profiles for Ru and O were measured by RBS. The spectrum shows that the oxygen is uniformly distributed

(22) Kay, J. G.; Green, D. W.; Duca, K.; Zimmerman, G. L. *J. Mol. Spectrosc.* **1989**, *138*, 49–61.

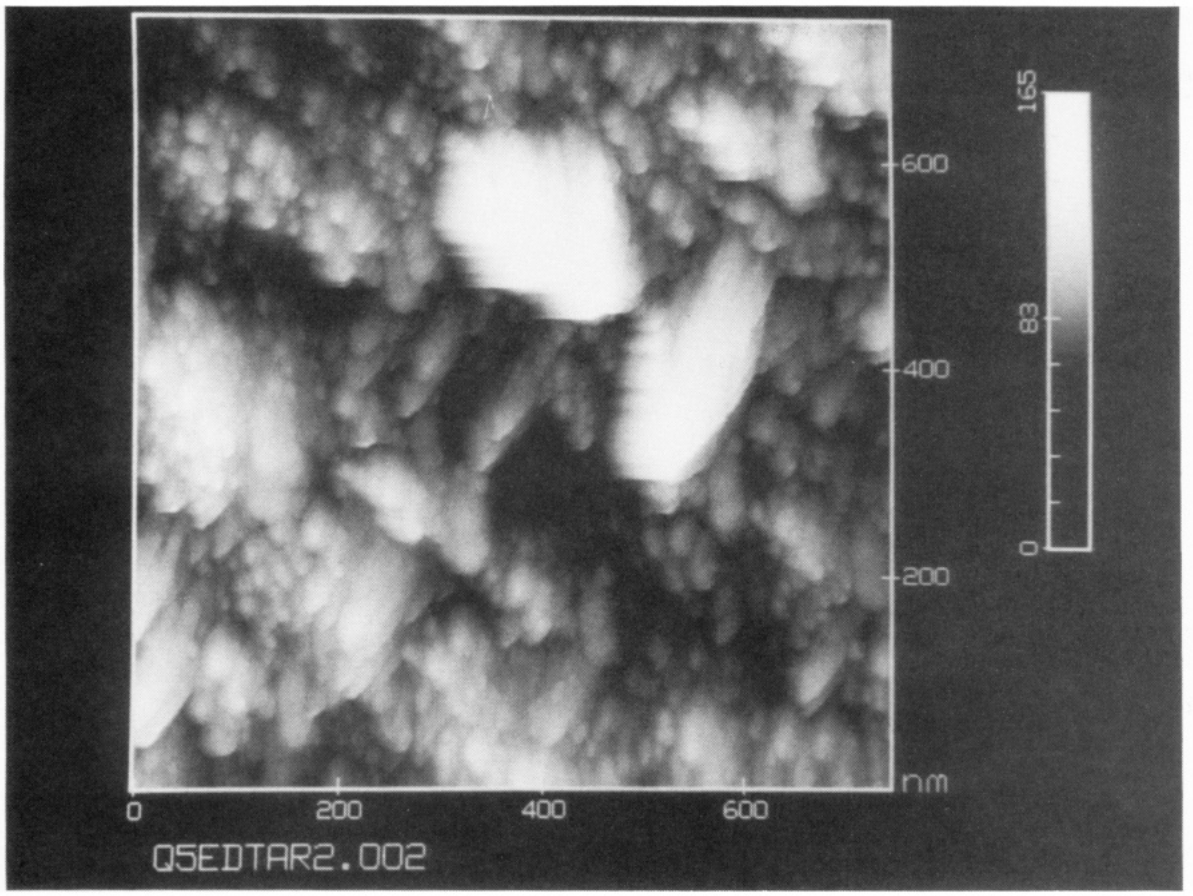

Figure 3. A 800 nm × 800 nm top view STM image of a Ru thin film in air. Domains of approximately 100–150 nm are clearly resolved and consist of smaller subunits of about 10–25 nm in size.

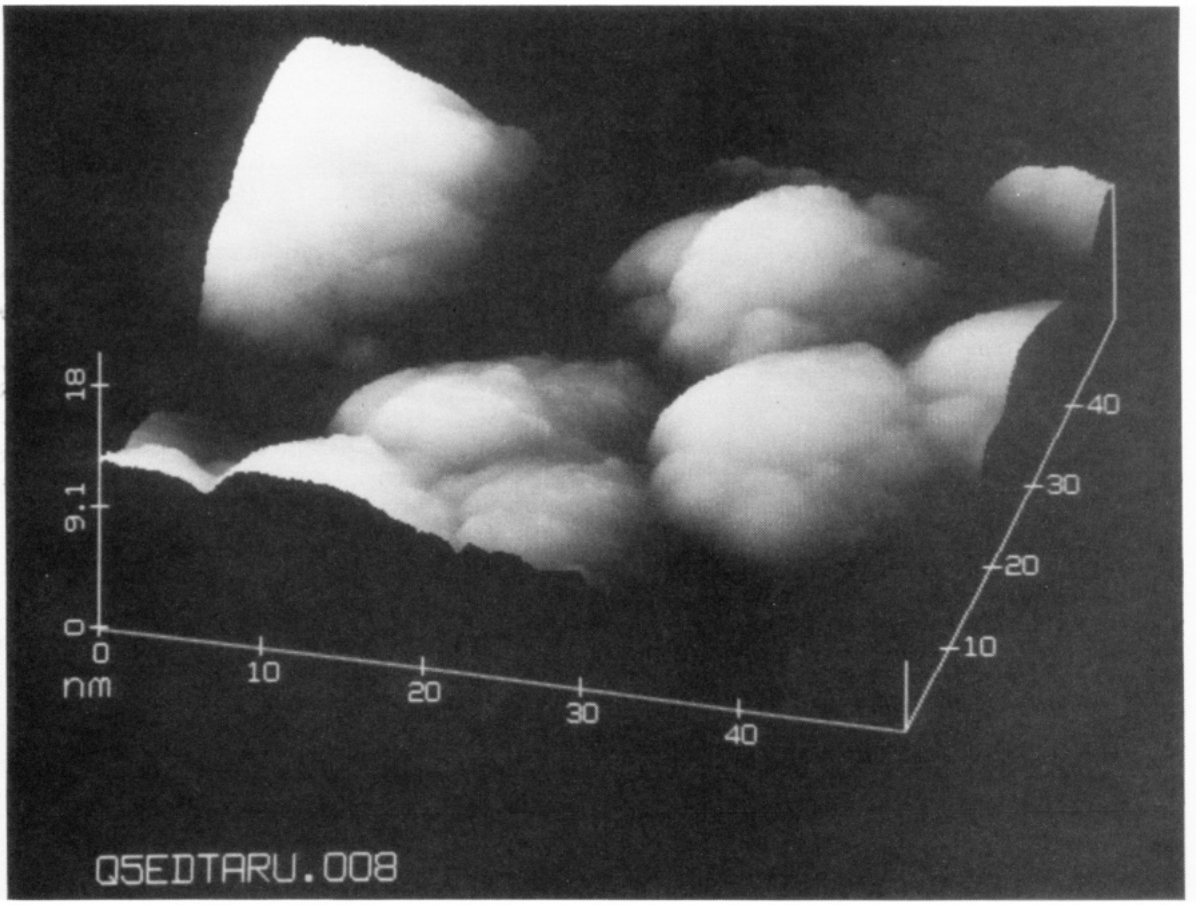

Figure 4. Higher resolution (50 nm × 50 nm) side view (30°) STM constant-current image of the same film as in Figures 2 and 3.

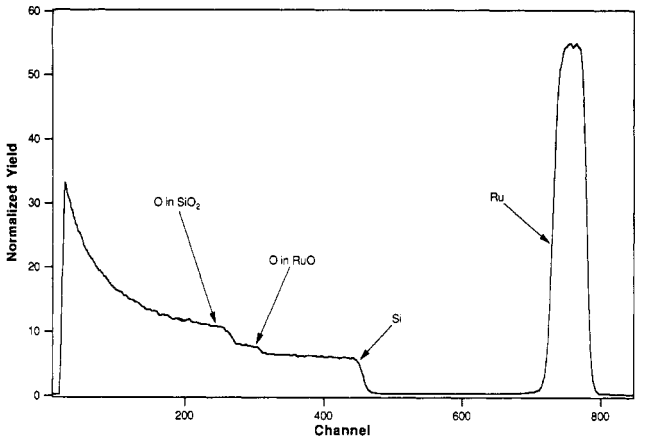

Figure 5. RBS spectrum of a metallic ruthenium mirror thin film on a fused-quartz substrate.

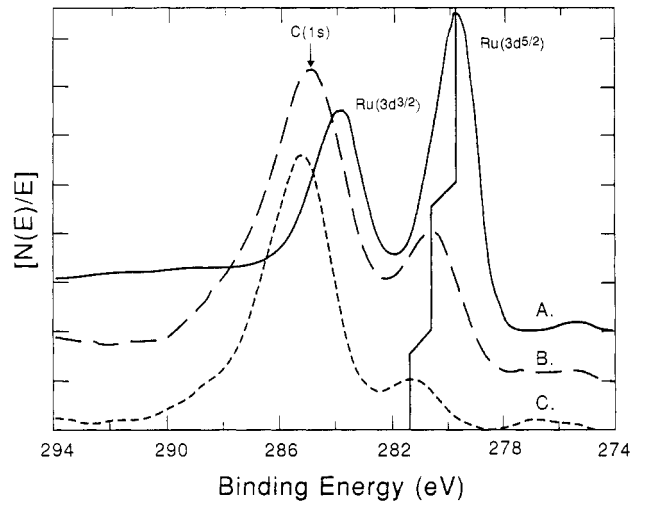

Figure 6. XPS spectrum of the C(1s) and Ru(3d) region for (A) the metallic Ru mirror thin film, (B) the [TMPEDTA]Ru^{II}Pz powder, and (C) the covalently attached [TMPEDTA]Ru^{II}Pz complex, where Pz = pyrazine.

in the films. Carbon and nitrogen peaks are not observed in the 2.2 MeV RBS spectra due to the large oxygen background from the fused silica substrates and the low scattering cross section at a He^+ beam energy of 2.2 MeV, indicating that the amount of these elements present are less tha 2–3%, the detection limit of RBS. Because of low scattering cross sections for light elements, RBS is appropriate only for quantitative determination of elements of $Z > 10$ and has limited use for light elements in heavy-element matrix.[23] Direct measurement of the oxygen content of these materials is also complicated by the large oxygen background.

Electron microprobe analysis (EMPA) of these materials is complicated by the SiO_2 substrate. Therefore, direct quantitative measurements are not possible. Film thicknesses determined by EMPA agree well with those measured by RBS.

XPS data taken from the lightly sputtered cleaned "metallic" film indicated that the Ru was predominantly present in a metallic state ($3d^{5/2}$ transition at 279.7 eV). Figure 6 presents the XPS spectrum of the ruthenium metallic thin film in comparison with the monolayer of ruthenium TMPEDTA complex. The metallic Ru shows its characteristic binding energy at 279.7 eV and 283.8 eV

(23) Briggs, D.; Seah, M. P. In *Practical Surface Analysis by Auger and X-ray Photoelectron Spectroscopy*; Wiley: New York, 1983; Chapter 4, pp 141–179.

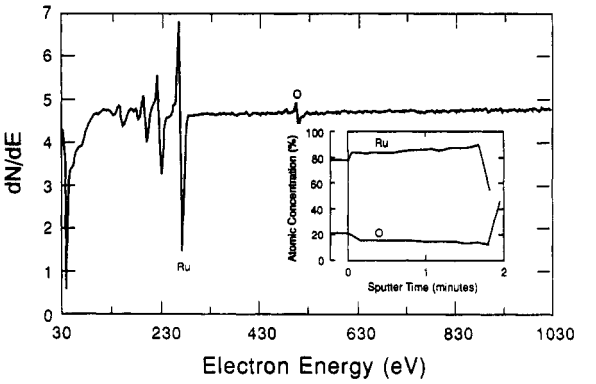

Figure 7. Representative differential AES spectrum, dN/dE versus electron energy, recorded in the interior of the metallic Ru mirror film. Inset: depth profiles of the same surface.

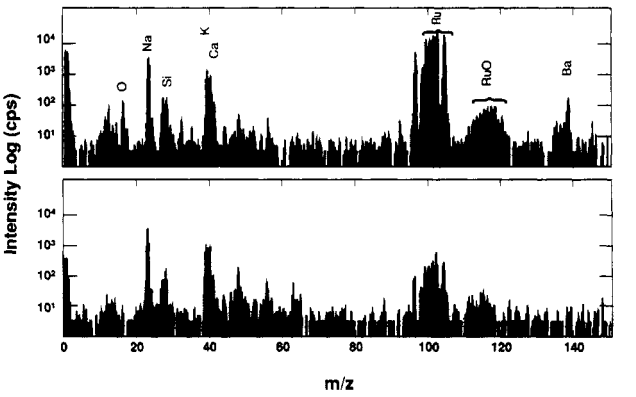

Figure 8. Positive SIMS spectra of pure Ru metal (top) and solution grown Ru mirror thin film from thermal disproportionation reaction of $Ru(H_2O)_6^{2+}$.

corresponding to $Ru^{5/2}$ and $Ru^{3/2}$, respectively. The intensity ratio of $Ru^{5/2}$ and $Ru^{3/2}$ is roughly 3:2, which matches well with pure ruthenium, and this further indicates that the chemical composition of this thin film is mainly ruthenium. A significant concentration of O (0.08–0.18 a/o) was observed in the film from AES and SIMS depth profiles. In the positive ion SIMS depth profiles, high carbon contaminant and relatively low ruthenium yield on the very outer surface was observed. The carbon ions decreased rapidly and reached a steady state after about 200 s of sputtering time. A representative carbon signal increase at the interface of ruthenium mirror film and fused quartz was found after sputtering the metallic film for approximately 1200 s while the intensity of Si and SiO ions began to increase and Ru ions started falling. This carbon signal is due to the TMPEDTA adhesion monolayer first introduced onto the silica surfaces. The SIMS profile results confirm that the TMPEDTA ligand is still present at the interface of the Ru film and the quartz substrate (i.e., increase in C and N positive ion yield seen when sputtering with deliberately high O_2 gas pressure ($P_{O_2} = 3.3 \times 10^{-7}$ mbar)).

A representative differential AES spectrum recorded in the interior of the film is shown in Figure 7, along with the depth profile (inset). As illustrated in Figure 7, the metallic Ru feature in the region of 130–255 eV is predominant. Furthermore, the Auger differential spectrum suggests a low concentration of oxygen (see O Auger electron at 500 eV in Figure 7) in these ruthenium thin films. The inset Auger depth profiles (see Figure 7) have the same features as those of the positive ion SIMS profiles, e.g., low Ru concentration and high contaminant at the very metallic outer surface. The oxygen content also manifests itself in higher ion counts from the static SIMS

spectra recorded in the interior of the solution grown ruthenium film when compared to a static SIMS positive ion spectrum recorded from sputtered cleaned metallic Ru as illustrated in Figure 8. The two major features in Figure 8 are the species corresponding to the mass of Ru and RuO. Ruthenium has seven natural isotopes and their natural abundances in percent are as follows: ^{96}Ru, 5.5; ^{98}Ru, 1.9; ^{99}Ru, 12.7; ^{100}Ru, 12.6; ^{101}Ru, 17.1; ^{102}Ru, 31.6; ^{104}Ru, 18.6. The observed ion intensity distribution shown in Figure 8 for both Ru ions and RuO ions matches perfectly with the ruthenium natural abundance pattern. The ruthenium in the metallic thin film appears to be much purer than commercially available ruthenium metal as is indicated in Figure 7 by the fact that the SIMS spectrum of the Ru thin film lacks a feature at m = 137 which was assigned to barium. The observation of suboxide RuO fragments indicates the presence of Ru–O bonds in the Ru mirror films. Masses corresponding to ruthenium dioxide and trioxide were not found in these metallic mirror thin films.

Conclusions

Smooth, shiny, metallic Ru mirrors were successfully fabricated via a TMPEDTA adhesion layer between the interface of Ru and fused quartz. The chemical composition of these Ru mirrors was analyzed by AEP, XPS, SIMS, and RBS, and these surface characterizations indicate that the thin metallic film consists of mainly Ru metal. Infrared spectroscopy reveals that the Ru mirrors reflect infrared radiation perfectly; therefore, application of these low-cost Ru mirrors in infrared instruments is plausible. The smoothness suggested by STM and SEM is far below the order of micrometers, which implies that the Ru mirrors are extremely smooth to light waves in the infrared region.

Registry No. TMPEDTA, 84127-79-7; $Ru(H_2O)_6^{2+}$, 30251-71-9; SiO_2, 60676-86-0; Ru, 7440-18-8; Si, 7440-21-3.

Mixed-Metal Amorphous and Spinel Phase Oxidation Catalysts: Characterization by X-ray Diffraction, X-ray Absorption, Electron Microscopy, and Catalytic Studies of Systems Containing Copper, Cobalt, and Manganese

Paul A. Wright,* Srinivasan Natarajan, and John M. Thomas*

The Davy Faraday Research Laboratory, The Royal Institution of Great Britain, 21 Albemarle Street, London W1X 4BS, UK

Pratibha L. Gai-Boyes

Central Research & Development, E. I. Du Pont de Nemours, Experimental Station, Wilmington, Delaware 19880-0356

Received April 1, 1992. Revised Manuscript Received June 8, 1992

Mixed-metal carbonates $CuMn_2(CO_3)_3$, $CuMn(CO_3)_2$, $CoMn_2(CO_3)_3$, and $CuCoMn(CO_3)_3$ possessing the rhodocrosite structure have been prepared by coprecipitation. Extended X-ray absorption fine structure (EXAFS) analysis indicates that cobalt substitutes fully and without distortion into the rhodocrosite structure in $CoMn_2(CO_3)_3$, whereas copper is present in $CuMn_2(CO_3)_3$ in a distorted environment. Decomposition at temperatures of ca. 600 K for $CuCoMn(CO_3)_3$ and ca. 690 K for the other carbonates yields amorphous or (for the $CoMn_2$ system) very poorly crystalline oxides. EXAFS analyses of these solids reveals that cobalt and manganese ions order to the second and higher coordination shells in proto-spinel structures faster than do ions of copper. The majority of manganese and cobalt cations have 6-fold and most copper 4-fold coordination in the just-decomposed oxides, although in the poorly crystalline $CoMn_2$ oxide around one-third of the cobalt ions are in tetrahedral sites. Heating the carbonates to 773 K in air produces spinels that are phase pure by X-ray diffraction: whereas the copper-bearing spinels are cubic, $CoMn_2O_4$ is tetragonal. Copper occupies mainly tetrahedral sites in these spinels, although the presence of some octahedral copper is clearly revealed by EXAFS. This increases in the order $CuCoMnO_4 < CuMn_2O_4 < Cu_{1.5}Mn_{1.5}O_4$. Manganese is predominantly octahedral in all of the spinels (Jahn–Teller distortion in $CoMn_2O_4$) and cobalt is octahedral in $CuCoMnO_4$ and occupies both sites in $CoMn_2O_4$, ordering on to the tetrahedral site upon heating. On the basis of EXAFS and X-ray absorption near-edge spectral (XANES) analyses and assuming the spinels are stoichiometric, we infer that copper is present in the spinels as a mixture of 1+ and 2+ ions. In $CuMn_2O_4$ and $CuCoMnO_4$ the manganese is present as a mixture of 3+ and 4+ and in $CoMn_2O_4$ predominantly as 3+. Cobalt is 3+ in $CuCoMnO_4$ and a mixture of 2+ and 3+ in $CoMn_2O_4$. Many of the oxides catalyze the complete reaction of an undiluted 2:1 CO/O_2 gas mixture at room temperature, so that dilution of both the gas mixture and the catalyst itself was performed to give conversions less than 100% between 60 and 160 °C. Amorphous oxides in the Cu/Mn and Co/Mn systems have slightly higher specific activities than the corresponding spinels. Of all the mixed-metal oxides prepared, the $CuCoMnO_4$ spinel has both the highest specific activity, probably due to the cobalt being largely trivalent, as well as the highest surface area.

Introduction

The ability of amorphous manganese oxides promoted by transition metals to catalyze the oxidation of carbon monoxide and hydrocarbons, even at ambient temperature, has long been known.[1] Amorphous manganese oxide with added copper, known as hopcalite, has been studied to

(1) Jones, H. A.; Taylor, H. S. *J. Phys. Chem.* **1923**, *27*, 623.

0897-4756/92/2804-1053$03.00/0